Degradation mechanism of organic photovoltaic devices with bathocuproine buffer layer

Chih-Chien Lee
Wei-Cheng Su
Jia-Cing Huang
Chi-Feng Lin
Shun-Wei Liu

Degradation mechanism of organic photovoltaic devices with bathocuproine buffer layer

Chih-Chien Lee,[a] Wei-Cheng Su,[b] Jia-Cing Huang,[c] Chi-Feng Lin,[d] and Shun-Wei Liu[e]

[a] National Taiwan University of Science and Technology, Department of Electronic Engineering, 43, Section 4, Keelung Road, Taipei, 106, Taiwan

[b] National Taiwan University of Science and Technology, Graduate Institute of Electro-Optical Engineering, 43, Section 4, Keelung Road, Taipei, 106, Taiwan

[c] National Taiwan University of Science and Technology, Department of Electronic Engineering, 43, Section 4, Keelung Road, Taipei, 106, Taiwan

[d] National Taiwan University, Graduate Institute of Photonics and Optoelectronics, 1, Section 4, Roosevelt Road, Taipei, 10617 Taiwan

[e] Academia Sinica, Institute of Chemistry, 128 Academia Road, Section 2, Nankang, Taipei 115, Taiwan

cclee@mail.ntust.edu.tw

Abstract. The degradation mechanism of pentacene/fullerene (C_{60})-based photovoltaic device is studied as a function of heating time. The efficiency of the device with bathocuproine (BCP) as buffer layer shows a considerable decay from 1.49 to 0.6% after 168-h heating, whereas the device without BCP possessed a stable performance under heating treatment. This decay is mainly caused by the poor thermal stability of BCP, which crystallized after the heating treatment and is discussed through the incident photon-to-electron conversion efficiency (IPCE) and the atomic force microscopic (AFM) measurements. The IPCE results indicated the redistribution of optical field due to the crystallization of BCP, and the AFM images showed the significant increase in surface root-mean-square value from 0.46 to 24.7 nm. Furthermore, the device without BCP exhibited the decrease in series resistance (R_s). The reduced R_s was attributed to the polycrystallized-like molecular arrangement after heating, which was confirmed by the Gaussian-disordered model. © *2011 Society of Photo-Optical Instrumentation Engineers (SPIE)*. [DOI: 10.1117/1.3555079]

1 Introduction

The organic semiconductors were widely used on solar cells, light-emitting diodes, thin-film transistors, and memories due to the potential for flexibility and ease of process. In contrast to the inorganic photovoltaic (PV) devices, the organic ones possess a high absorption coefficient for generating more excitons. The carrier diffusion length, however, is much shorter for organic materials than that for inorganic ones therefore limits the performance. To date, many efforts for improving organic PV (OPV) performance have been made and the power-conversion efficiency (PCE) was much higher than the earlier OPV devices presented by Tang.[1] For instance, various blocking layers (EBLs) were studied for choosing a suitable material to improve the PCE due to the fact that the EBL was suggested to be a barrier for preventing exciton quenching and an effective electron transporting layer.[2–5] The electrode of OPV devices was believed to

influence the open-circuit voltage (V_{OC}) significantly[6] and investigated to obtain the better carrier extraction.[7–10] At the same time, the effects of EBL and electrode materials on degradation were verified. Song et al. elongated the lifetime of OPV devices by 150 times with changing EBL from bathocuproine (BCP) to tris-(8-hydroxyquinoline) aluminum (Alq$_3$).[11] Reese et al. inspected the various cathode types and proposed that the interaction of organic materials and metal atoms greatly affects the lifetime.[12] There were other research focusing on the stability of OPV devices in either a small-molecule or polymer-based system.[13–17] The common degraded mechanisms were the oxidation of materials, such as the diffusion of oxygen into organic materials resulting in the reduction in mobility, hence, poor carrier transport,[18–22] and the reduced π conjugation and chain scission of polymer as a result from the photodegradation.[23] This indicated that the influence of ambient atmosphere, such as oxygen and water, plays an important role on device degradation. With this point of view, the insulation of organic materials from the ambient atmosphere could improve the device lifetime by well encapsulation. It has been demonstrated that, with the encapsulation using Al$_2$O$_3$ by atomic layer deposition, the pentacene/fullerene (C$_{60}$)-based OPV devices could maintain the PCE in air over 6000 h,[24] which was much longer than the lifetime of OPV devices in previous reports.

Despite the ambient effect on device degradation, the change of the interfacial properties as a result from the annealing treatment provided different degradation mechanism.[25] In this paper, we demonstrate the degradation process for the pentacene/C$_{60}$-based heterojunction devices, both with and without BCP, with well encapsulation at high temperature similar to the practical operating condition under solar illumination. One reason for the degradation of devices with BCP was suggested to be the crystallization of BCP.[26] Such morphological change caused by crystallization of BCP was explained by the incident photon-to-electron conversion efficiency (IPCE) measurement and atomic force microscopic (AFM) images. Other degradation mechanisms are also discussed for both devices without BCP.

2 Experimental

The devices were fabricated on the indium-tin-oxide (ITO) substrates. After the solvent cleaning, the substrates were transferred into the vacuum chamber, then the organic layer and metal were deposited through thermal deposition under high-vacuum condition (about 8×10^{-6} Torr). The active layer consisted of pentacene and C$_{60}$ as the donor and acceptor, respectively. The deposition rate was controlled in 0.1–0.2 nm/s, which was monitored by the quartz crystalline microbalance. Two kinds of devices were used, one is the device with 10 nm BCP interposed between active layer and cathode metal as a buffer layer, another one is the device without BCP. After the deposition of the Al, the organic materials that served as the cathode were deposited in the same chamber through a shadow mask, which defined the active area as 0.04 cm^2. After the thermal deposition process, the devices were transferred into the glove box and encapsulated under nitrogen atmosphere to prevent the influence of water and oxygen. Finally, the device without BCP layer was preannealed prior to the measurements, whereas the device with BCP was not subjected to any treatment. The current-voltage (J–V) characteristic measurement was performed in air under 1-sun AM 1.5G-simulated solar illumination (Newport Model 91160A), which was calibrated by a silicon reference cell (PV Measurement, Inc.).

The investigation of a lifetime was conducted as follows. Two kinds of devices, with and without BCP, were placed on a hot plate and heated at constant temperature of 60°C in nitrogen atmosphere. The J–V characteristic was carried out in air every 24 h. The performance after being preannealed for 168 h was chosen as the initial efficiency of the devices without BCP. The initial efficiency of the device with BCP before heating was chosen as the reference point.

For the IPCE measurement, the AM 1.5G solar simulator was used to generate the bias light. A monochromator (Newport Model 74100), which was calibrated with a National Institute of Standards and Technology (NIST) calibrated photodiode and chopped at 250 Hz, was used to select the wavelengths between 400 and 800 nm for illuminating the OPV device. The photocurrent from the OPV device was measured through the lock-in amplifier (Signal Recovery

7265), which was in turn referenced to the chopper frequency. To confirm the IPCE data, the AM 1.5G spectrum was then used to obtain short-circuit current density (J_{SC}) and the error value was ~4%, compared to the current density measured under solar simulator illumination. All electrical measurements were carried out in air.

The samples for AFM measurement were prepared onto ITO glass substrates. The organic films, pentacene, C_{60}, and BCP were deposited onto separate substrates and then the samples were placed on a hot plate to be heated at 60°C. The images were obtained with a Park System XE-100 in ambient atmosphere, with noncontact mode and resonance frequency of 6×10^4 Hz.

3 Results and Discussion

Figure 1(a) shows the normalized efficiency of two kinds of devices, with and without BCP, as a function of heating time. The device without BCP exhibits a stable performance after 168-h heating, whereas the device with BCP decays rapidly and the efficiency is dropped from 1.49 to 0.6%. These results indicate that the insertion of BCP between the active layer and cathode plays an important role on the device degradation mechanism because the devices were well encapsulated to prevent the influence of ambient atmosphere. The detailed electrical properties of the devices could be discussed through the J–V characteristics of the devices as depicted in Fig. 1(b), which represents the initial condition (0 h) and final condition (168 h) for the both devices, respectively. The device without BCP achieves similar performance to the device with BCP after being preannealed for 168 h. The drop in J_{SC} and the reduction of fill factor (FF) is observed for the device with BCP at the final condition, whereas the V_{OC} remained the same. The reduction of FF could be attributed to the increased series resistance (R_s) and the decreased shunt resistance (R_{sh}). The drop in J_{SC} is reasonable to be subjected to the crystallization of BCP after heating treatment.

The J–V characteristic parameters are depicted in Figs. 2(a) and 2(b) for the device with and without BCP, respectively. The device with BCP is considered first. The R_{sh} is decreased from 0.33 to 0.16 kΩ cm^2, and as a result, the FF is reduced from 50.1 to 35.3%. The decrease in R_{sh}, which represents the increased carrier recombination, could be attributed to the poor carrier injection (extraction) at the organic/metal interface due to the crystallization of BCP. The changeless V_{OC} implies the invariance of the built-in potential inside the device and the energy offset between anode and cathode. The J_{SC} is diminished from 7.1 to 3.9 mA/cm^2, which corresponds to the recombination of carriers and the poor contact at the interface. The overall PCE is dropped from 1.49 to 0.69% because of the reduction of FF and J_{SC}. In contrast, the device without BCP shows a stable performance after achieving the highest efficiency by being preannealed. It could be ascribed to the absence of the BCP layer, hence no morphological change at the organic/metal interface.
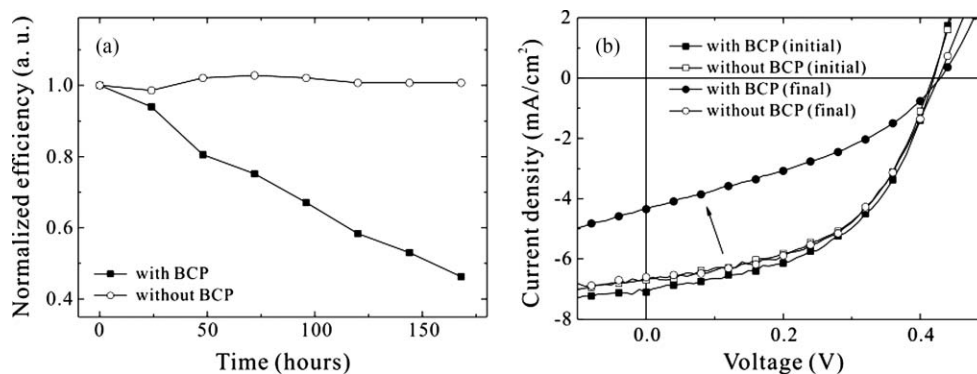

Fig. 1 (a) Normalized efficiency of the device with and without BCP as a function of heating time and (b) J–V curves of both devices at 0 h (initial) and 168 h (final).
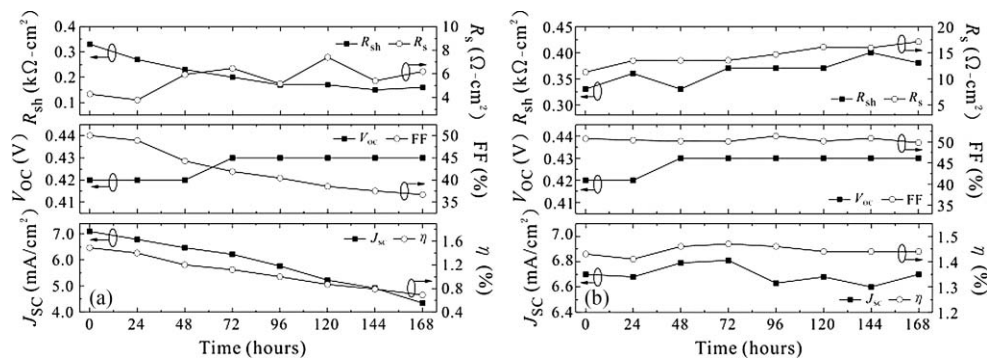
Fig. 2 Electrical parameters of the device (a) with BCP and (b) without BCP as a function of heating time.

The IPCE spectra of the two devices are shown in Figs. 3(a) and 3(b) for the device with and without BCP, respectively. As our expectation, the IPCE spectrum of the device without BCP is unchanged after the heating treatment due to the absence of BCP. This result is consistent with the stable performance in the electrical properties previously discussed. The IPCE spectrum of the device with BCP, however, decays from about 55 to 30% at 665 nm. The decrease in IPCE spectrum corresponds to the reduction of J_{SC}. The normalized IPCE spectrum shows a significant increase at the final condition within the range from 400 to 550 nm. This enhancement in the IPCE spectrum of the device with BCP is attributed to the redistribution of optical field inside the device, which was believed to be responsible for the photocurrent spectrum.[27] Moreover, the influence of shorter wavelength range on the optical field distribution is more significant than that of longer wavelength.[28] Therefore, it could be suggested that the crystallization of BCP results in the change of the optical field distribution, which enhances the IPCE spectrum of device with BCP in the shorter wavelength range.

Further analysis of the morphology at the interfaces between organic/organic and organic/metal is done by the AFM images as shown in Fig. 4. Figure 4(a) presents the film surface of pentacene as deposited and after heating treatment. It could be noted that no significant change is observed for the pentacene film. Similarly, the C_{60} film displays only a slight difference in surface before and after heating as indicated by Fig. 4(b). Combining the two results discussed above could give the presumption that the interfacial property at the donor–acceptor interface was not altered during the heating treatment. Therefore, the dissociation of excitons is consequently undisturbed. The morphological property of BCP is also studied, as shown in Fig. 4(c). The average root-mean-square (rms) value of the surface roughness for pristine BCP
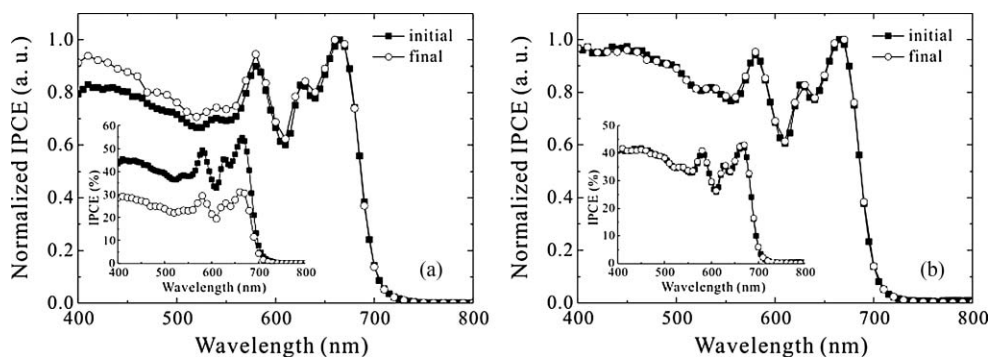

Fig. 3 Normalized IPCE spectra of the devices (a) with BCP and (b) without BCP. Insets show the IPCE spectra without normalizing.
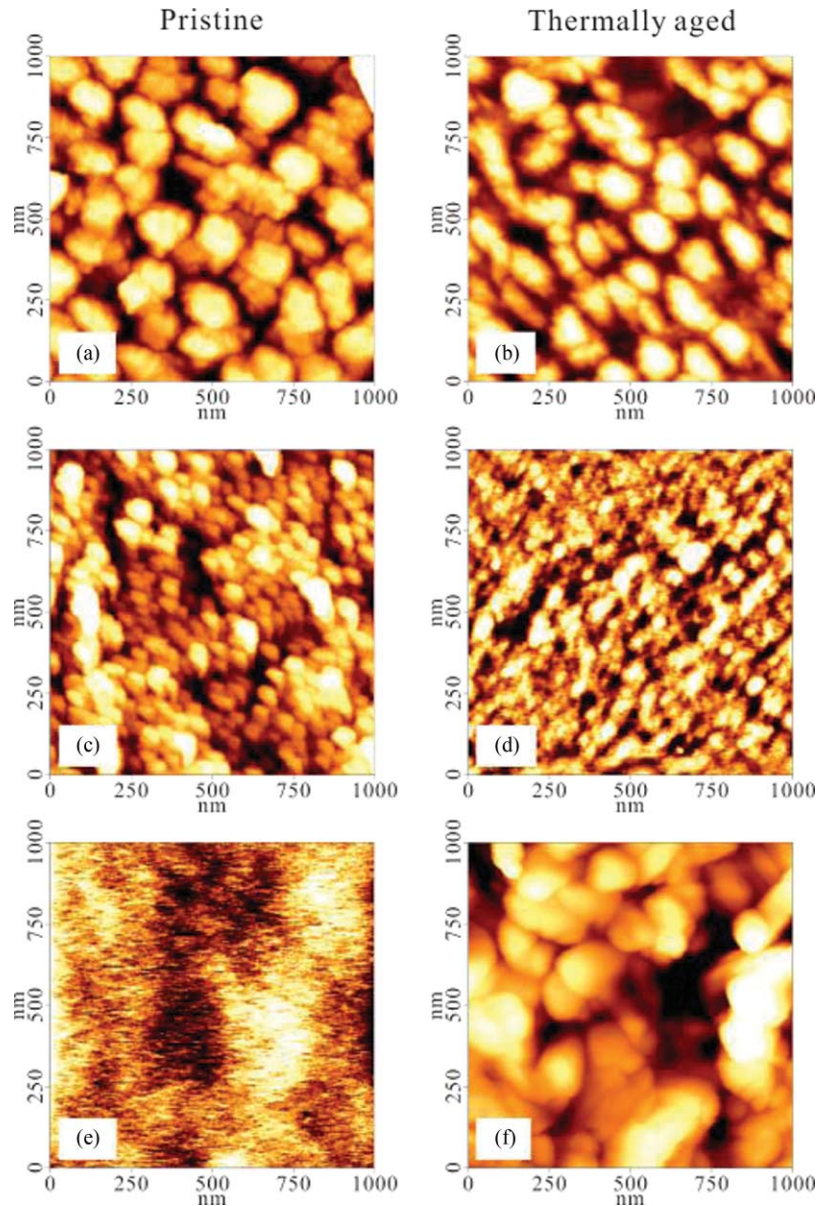
Fig. 4 AFM images of (a, b) pentacene, (c, d) C_{60}, and (e, f) BCP thin films. (a, c, e) shows the pristine films as-deposited before being thermally aged and (b, d, f) shows them after being thermally aged.

film is 0.46 ± 0.02 nm, while the rms value for heated BCP surface is 24.7 ± 0.2 nm. Obviously, the surface roughness increases after heating treatment owing to the crystallization of BCP. The emergence of the islandlike morphology may result in the delamination in both interfaces BCP/Al and C_{60}/BCP. It explains the drop in J_{SC} due to the reduced effective electrical area between BCP and Al interface, which is responsible for electron collection and injection. The poor contact at the interface leads also to the increase in R_s and the decrease in R_{sh} and, hence, the FF. Most importantly, the reduced effective electrical area at which the currents pass through might cause the Joule heating to make the accelerated degradation at the BCP/Al interface. In our previous reports, the optical absorption method has been completely confirmed this finding and morphology issues in case of C_{60}/BCP/Al have been addressed.[29]
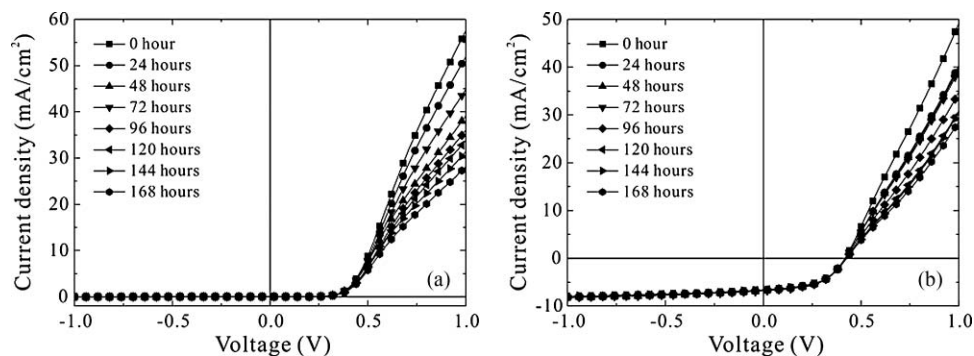
Fig. 5 The *J–V* characteristics of the device without BCP (a) in dark and (b) under illumination.

Returns to the *J–V* characteristics swept from –1 to 1 V for the device without BCP in dark and under illumination, as shown in Figs. 5(a) and 5(b), respectively. The *J–V* curves in the fourth quadrant under illumination keep almost the same shape after heating for 168 h. In the first quadrant, however, a weird reduction in injection current is observed. It could be attributed to the increase in the R_s, which is characterized by the resistivity of each organic material and the interfacial barrier at the electrodes. The latter is not likely to the factor of increasing R_s due to the same turn-on voltage for all the *J–V* curves at different heating time. It could contribute the increased R_s to the increased resistivity of organic layer after heating treatment. To understand the factor to the increased resistivity, the Gaussian disorder model[30] (GDM) was given as follows:

$$\mu(T, E) = \mu_0 \exp\left\{-\left(\frac{2\sigma}{3kT}\right)^2 + C_0\left[\left(\frac{\sigma}{kT}\right)^2 - \Sigma^2\right]\sqrt{E}\right\},$$

where T is the temperature, E is the electric field, μ_0 is the mobility prefactor, σ and Σ are parameters representing the degree of energetic and spatial disorder, and C_0 is an empirical constant that depends on the intersite distance. This equation reveals that the mobility depends on the applied electric field and spatial disorder. Under high electric-field condition, the mobility is dominated by the spatially diordered constant, whereas in the short-circuit condition (no applied electric field), the mobility remained constant. The heating treatment supplies an additional energy to redistribute the organic materials and form polycrystal structure (i.e., the more spattial disorder is produced, therefore reducing the mobility). The high R_s due to the decreased mobility after heating is consistent with the GDM equation shown above.

4 Conclusion

The degradation mechanism of the OPV device based on pentacene/C_{60} was discussed. The efficiency of the device with BCP decayed from 1.49 to 0.6% after 168-h heating, whereas the device without BCP showed a stable performance under the same treatment. The crystallization of BCP after heating treatment was observed through the IPCE and AFM measurements. The IPCE results showed the redistribution of optical field, and the AFM images further confirmed the crystallization of BCP by a significant increase in surface rms value. It could be inferred that the degradation was mainly due to the poor thermal stability of BCP. It resulted in the delamination of BCP and Al interface, which caused the reduced effective electrical area. The reduced effective electrical area led to the Joule heating at the interface and accecelarated the degradation of the device with BCP. Furthermore, the heating treatment induced the formation of polycrstalline of organic layer and hence reduced the electric-field dependent mobility in the device without BCP.

Acknowledgments

References

1. C. W. Tang, "Two-layer organic photovoltaic cell," *Appl. Phys. Lett.* **48**, 183–185 (1986).
2. P. Peumans, V. Bulović, and S. R. Forrest, "Efficient photon harvesting at high optical intensities in ultrathin organic double-heterostructure photovoltaic diodes," *Appl. Phys. Lett.* **76**, 2650–2652 (2000).
3. B. P. Rand, J. Li, J. Xue, R. J. Holmes, M. E. Thompson, and S. R. Forrest, "Organic double-heterostructure photovoltaic cells employing thick tris(acetylacetonato)ruthenium(III) exciton-blocking layers," *Adv. Mater.* **17**, 2714–2718 (2005).
4. M. Vogel, S. Doka, Ch. Breyer, M. Ch. Lux-Steiner, and K. Fostiropoulos, "On the function of a bathocuproine buffer layer in organic photovoltaic cells," *Appl. Phys. Lett.* **89**, 163501 (2006).
5. M. Y. Chan, C. S. Lee, S. L. Lai, M. K. Fung, F. L. Wong, H. Y. Sun, K. M. Lau, and S. T. Lee, "Efficient organic photolvaic devices using a combination of exciton blocking layer and anodic buffer layer," *J. Appl. Phys.* **100**, 094506 (2006).
6. K. Kawano, N. Ito, T. Nishimori, and J. Sakai, "Open circuit voltage of stacked bulk heterojunction organic solar cells," *Appl. Phys. Lett.* **88**, 073514 (2006).
7. C. J. Brabec, S. E. Shaheen, C. Winder, N. S. Sariciftci, and P. Denk, "Effect of LiF/metal electrodes on the performance of plastic solar cells," *Appl. Phys. Lett.* **80**, 1288–1290 (2002).
8. E. Ahlswede, J. Hanisch, and M. Powalla, "Comparative study of the influence of LiF, NaF, and KF on the performance of polymer bulk heterojunction solar cells," *Appl. Phys. Lett.* **90**, 163504 (2007).
9. H.-H. Liao, L.-M. Chen, Z. Xu, G. Li, and Y. Yang, "Highly efficient inverted polymer solar cell by low temperature annealing of Cs_2CO_3 interlayer," *Appl. Phys. Lett.* **92**, 173303 (2008).
10. F.-C. Chen, J.-L. Wu, S. S. Yang, K.-H. Hsieh, and W.-C. Chen, "Cesium carbonate as a functional interlayer for polymer photovoltaic devices," *Appl. Phys. Lett.* **103**, 103721 (2008).
11. Q. L. Song, F. Y. Li, H. Yang, H. R. Wu, X. Z. Wang, W. Zhou, J. M. Zhao, X. M. Ding, C. H. Huang, and X. Y. Hou, "Small-molecule organic solar cells with improved stability," *Chem. Phys. Lett.* **416**, 42–46 (2005).
12. M. O. Reese, A. J. Morfa, M. S. White, N. Kopidakis, S. E. Shaheen, G. Rumbles, and D. S. Ginley, "Pathways for the degradation of organic photovoltaic P3HT:PCBM based devices," *Sol. Energy Mater. Sol. Cells* **92**, 746–752 (2008).
13. Q. L. Song, M. L. Wang, E. G. Obbard, X. Y. Sun, X. M. Ding, X. Y. Hou, and C. M. Li, "Degradation of small-molecule organic solar cells," *Appl. Phys. Lett.* **89**, 251118 (2006).
14. P. W. M. Blom, M. J. M. de Jong, and M. G. van Munster, "Electric-field and temperature dependence of the hole mobility in poly(*p*-phenylene vinylene)," *Phys. Rev. B* **55**, R656–R659 (1997).
15. H. Neugebauer, C. Brabec, J. C. Hummelen, and N. S. Sriciftci, "Stability and photodegradation mechanisms of conjugated polymer/fullerene plastic solar cells," *Sol. Energy Mater. Sol. Cells* **61**, 35–42 (2000).
16. T. Jeranko, H. Tributsch, N. S. Sariciftci, and J. C. Hummelen, "Patterns of efficiency and degradation of composite polymer solar cells," *Sol. Energy Mater. Sol. Cells* **83**, 247–262 (2004).

17. K. Kawano, R. Pacios, D. Poplavskyy, J. Nelson, D. D. C. Bradley, and J. R. Durrant, "Degradation of organic solar cells due to air exposure," *Sol. Energy Mater. Sol. Cells* **90**, 3520–3530 (2006).

18. A. Hamed, Y. Y. Sun, Y. K. Tao, R. L. Meng, and P. H. Hor, "Effects of oxygen and illumination on the *in situ* conductivity of C_{60} thin films," *Phys. Rev. B* **47**, 10873–10880 (1993).

19. B. Pevzner, A. F. Hebard, and M. S. Dresselhaus, "Role of molecular oxygen and other impurities in the electrical transport and dielectric properties of C_{60} films," *Phys. Rev. B* **55**, 16439–16449 (1997).

20. R. Könenkamp, G. Priebe, and B. Pietzak, "Carrier mobilities and influence of oxygen in C_{60} films," *Phys. Rev. B* **60**, 11804–11808 (1999).

21. M. Yamada, I. Ikemoto, and H. Kuroda, "Photooxidation of the evaporated films of poly-cyclic aromatic hydrocarbons studied by X-ray photoelectron spectroscopy," *Bull. Chem. Soc. Jpn.* **61**, 1057–1062 (1988).

22. A. Maliakal, K. Raghavachari, H. Katz, E. Chandross, and T. Siegrist, "Photochemical stability of pentacene and a substituted pentacene in solution and in thin films," *Chem. Mater.* **16**, 4980–4986 (2004).

23. M. S. A. Abdou and S. Holdcroft, "Mechanisms of photodegradation of poly(3-alkylthiophenes) in solution," *Macromolecules* **26**, 2954–2962 (1993).

24. W. J. Potscavage, S. Yoo, B. Domercq, and B. Kippelen, "Encapsulation of pentacene/C_{60} organic solar cells with Al_2O_3 deposited by atomic layer deposition," *Appl. Phys. Lett.* **90**, 253511 (2007).

25. K. Kawano and C. Adachi, "Evaluating carrier accumulation in degraded bulk heterojunction organic solar cells by a thermally stimulated current technique," *Adv. Funct. Mater.* **19**, 3934–3940 (2009).

26. P. Peumans, A. Yakimov, and S. R. Forrest, "Small molecular weight organic thin-film photodetectors and solar cells," *J. Appl. Phys.* **93**, 3693–3723 (2003).

27. L. A. A. Pettersson, L. S. Roman, and O. Inganäs, "Modeling photocurrent action spectra of photovoltaic devices based on organic thin films," *J. Appl. Phys.* **86**, 487–496 (1999).

28. S. Yoo, W. J. Potscavage Jr., B. Domercq, S.-H. Han, T.-D. Li, S. C. Jones, R. Szoszkiewicz, D. Levi, E. Riedo, S. R. Marder, and B. Kippelen, "Analysis of improved photovoltaic properties o pentacene/C_{60} organic solar cells: Effects of exciton blocking layer thickness and thermal annealing," *Solid-State Electron.* **51**, 1367–1375 (2007).

29. S. W. Liu, C. C. Lee, C. F. Lin, J. C. Huang, C. T. Chen, and J. H. Lee, "4-Hydroxy-8-methyl-1,5-naphthyridine aluminium chelate: a morphologically stable and efficient exciton-blocking material for organic photovoltaics with prolonged lifetime," *J. Mater. Chem.* **20**, 7800–7806 (2010).

30. D. Poplavskyy and J. Nelson, "Nondispersive hole transport in amorphous films of methoxy-spirofluorene-arylamine organic compound," *J. Appl. Phys.* **93**, 341–346 (2003).

Biographies and photographs of the authors are not available.